Frascati Physics Series Vol. XLV (2007) pp.217-224
Science with the New Generation of High Energy Experiments
Frascati, 18-20 June, 2007

GAMMA RAY ASTRONOMY WITH ARGO-YBJ: FIRST OBSERVATIONS

Silvia Vernetto [a,b]
for the ARGO-YBJ Collaboration

[a] *IFSI Torino, INAF, Italy*

[b] *INFN, Sezione di Torino, Italy*

Abstract

The ARGO-YBJ experiment is the first EAS detector combining a very high mountain altitude (4300 m a.s.l.) to a "full coverage" detection surface. These features allow ARGO-YBJ to work in the typical energy range of Cherenkov telescopes, with an energy threshold of a few hundreds GeV. The low threshold and the large field of view (∼2 sr) make ARGO-YBJ suitable to monitor the gamma ray sky, searching for unknown sources and unexpected events, like Active Galactic Nuclei flaring episodes or high energy Gamma Ray Bursts.

In this paper we present the preliminary results on Gamma Ray Astronomy obtained with the events collected in the first months of data taking, in particular the detection of gamma rays from the Crab Nebula, the observation of a Markarian 421 outburst in July-August 2006, and finally a search for Gamma Ray Bursts emission in the GeV energy range using the scaler mode technique.

1 The detector

ARGO-YBJ is an air shower detector optimized to work with an energy threshold of a few hundreds GeV. It is located at the Yangbajing Cosmic Rays Laboratory (Tibet, China) at an altitude of 4300 m above the sea level.

It consists of a 74×78 m^2 "carpet" realized with a single layer of Resistive Plate Counters (92% of coverage), operated in streamer mode, surrounded by a partially instrumented " sampling ring", for a total active area of 6700 m^2 (see Fig. 1). The detector is logically divided into 154 clusters, 130 of them forming the central carpet and 24 the sampling ring. The cluster, consisting of a set of 12 RPCs, is the basic DAQ unit of the detector. Signals from each RPCs are picked-up by 10 electrodes of dimension 56×62 cm^2 (the "pads") which provide the space-time pattern of the shower front with a time resolution of ~ 1 ns. Each pad is segmented into 8 strips (62×7 cm^2) which count the number of particles hitting the pad itself.

In order to extend the measurable primary energy range, the RPCs are equipped with 2 large size pads (140×125 cm^2), providing a signal of amplitude proportional to the number of particles.

The detector will be covered by a 0.5 cm thick layer of lead, in order to convert a fraction of the secondary gamma rays and to reduce the time spread of the shower front, increasing the angular resolution.

ARGO-YBJ operates in two independent acquisition modes: the "shower mode" and the "scaler mode".

In the "shower mode" all showers giving a number of fired pads $N_{pad} \geq N_{trig}$ in the central carpet during a time window of 420 ns are recorded. The spatial coordinates and the time of any fired pad are then used to reconstruct the position of the shower core and the arrival direction of the primary. To perform the time calibration of the 18480 pads, a software method had been developed[1].

Fig. 1 reports an example of a shower detected by the central carpet, showing the capability of ARGO-YBJ in providing a detailed view of the shower front.

The current trigger threshold $N_{trig} = 20$ corresponds to a primary gamma energy threshold of a few hundreds GeV, the exact value depending on the source spectrum and on the zenith angle of observation. With this trigger condition, the event rate is $\sim$4 kHz.

In the "scaler mode" the counting rates of each cluster are recorded every 0.5 s for 4 different levels of coincidence inside the cluster: ≥ 1, ≥ 2, ≥ 3, ≥ 4 pads, with a coincidence time window of 150 ns. The counting rates are respectively $\sim$40 kHz, $\sim$2 kHz, $\sim$300 Hz and $\sim$120 Hz per cluster, for the 4 coincidence levels.

This measurement allows the detection of secondary particles from very low energy showers (E>1 GeV) reaching the ground in a number not sufficient to trigger the detector operating in shower mode. In scaler mode the primary arrival directions are not reconstructed and the data are used to search for transient phenomena as Gamma Ray Bursts or Solar Ground Level Enhancements, and to study cosmic ray modulations due to the solar activity.

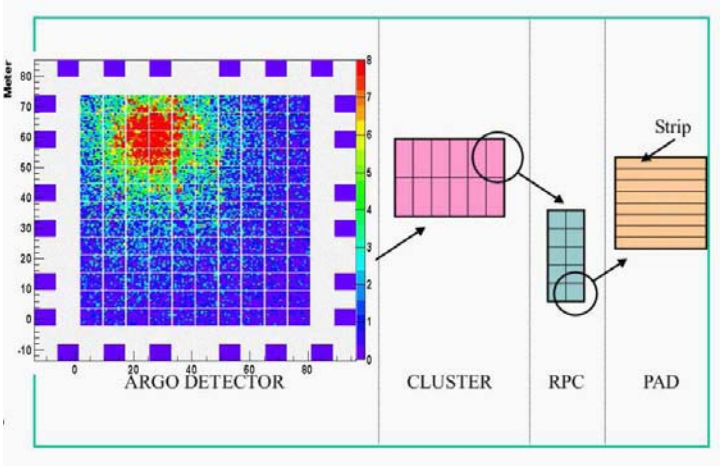

Figure 1: Layout of the ARGO-YBJ detector, with an example of a real shower superimposed to the central carpet. Each point represents a fired pad. Different colours indicate the number of fired strips per pad.

Since July 2006 the whole central carpet is in data taking. Preliminary results obtained with a subset of the data taken from July 2006 to March 2007 in shower mode and from December 2004 to March 2007 in scaler mode (with the detector surface increasing from $\sim$ 700 to $\sim$5600 m^2) are presented.

2 Detector angular resolution

The angular resolution has a statistical component, due to the fluctuations of the shower development and of the detector response, and a systematic one, arising from possible misalignment of the detector or systematic errors in the shower reconstruction.

Fig. 2 shows the angular resolution of ARGO-YBJ obtained by a Montecarlo simulation. The figure reports the value of Ψ_{72}, i.e. the angular difference between the true direction and the reconstructed one, as a function of the number of fired pads N_{pad}. Ψ_{72} is the radius of the circular window around the true direction containing 71.5% of the reconstructed events, which in the case of a gaussian point spread function is the radius of the observation window around a point source that maximizes the signal to noise ratio, and it is equal to 1.58 σ, where σ is the angular resolution. Ψ_{72} has been obtained by selecting the events with the reconstructed shower core inside the central carpet, for both primary gamma rays and protons [2]. The accuracy in the direction

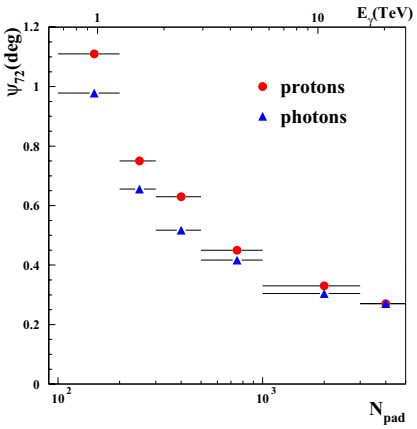

Figure 2: Angular resolution obtained by a Montecarlo simulation, comparing the true primary direction with the reconstructed one, for gamma rays and protons, as a function of N_{pad}. The upper scale gives the mean energy of gamma rays correspondent to a given N_{pad}, assuming a Crab-like spectrum.

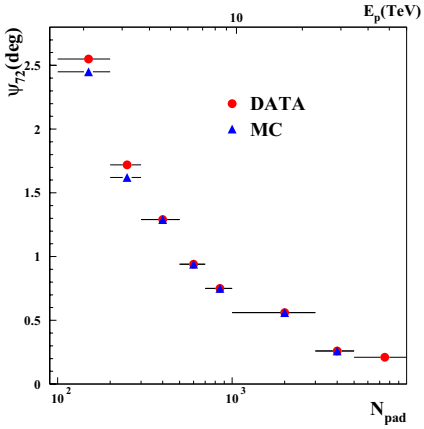

Figure 3: Measured angular difference in the shower direction reconstruction obtained with the "chessboard method", as a function of N_{pad}, compared with a Montecarlo simulation. The upper scale gives the mean energy of protons correspondent to a given N_{pad}, assuming a proton spectrum $\propto E^{-2.7}$.

determination increases with the number of pads. For $N_{pad} \geq 500$, Ψ_{72} is less than 0.5°.

A standard method to compare the simulated resolution with the real one, is the so called "even-odd" or "chessboard" method, consisting in splitting the detector in two parts (as the white and black squares of a chessboard) and comparing the arrival directions of showers independently obtained by the two detector subsets. Fig. 3 shows the opening angle Ψ_{72} between the two different reconstructions as a function of the number of fired pads, compared with Montecarlo expectation. The agreement is excellent (note that the "even-odd" angular difference given in Fig. 3 is expected to be a factor ∼2 larger than the one obtained with the full detector, given in Fig. 2).

The "even-odd" method allows to check only the statistical component of the angular resolution. To find out possible systematic effects it is common to study the profile and the position of the shadow that the Moon casts on the cosmic ray flux, the strongest "anti-source" of the sky.

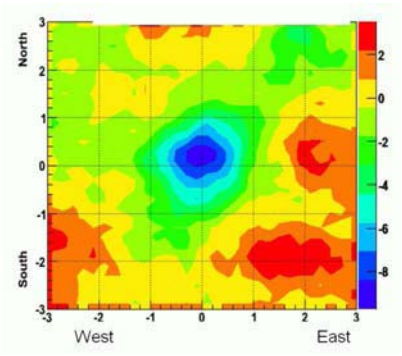

Figure 4: Map of the Moon region. The colour scale shows the significance of the shadow in standard deviations. The axes report the distance in degrees from the Moon position.

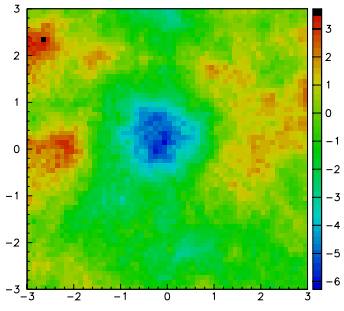

Figure 5: Map of the Sun region. The colour scale shows the significance of the shadow in standard deviations. The axes report the distance in degrees from the Sun position.

3 The Moon shadow

The Moon shadow is an important tool for ground-based detectors. The spread and the shape of the shadow at energies where the geomagnetic effect is small, provide a measurement of the angular resolution of the detector, and the position of the shadow allows to find out possible pointing biases.

To minimize the effects of the bending of cosmic rays in the geomagnetic field ($\sim 1.6^\circ$ /E(TeV) westward) we consider only the events with $N_{pad} \geq 500$, corresponding to a median energy of $\sim$5 TeV. Fig. 4 shows the significance map of the Moon shadow, obtained during 558 hours of observation, selecting the events with zenith angle $< 50^\circ$. A deficit of $\sim$10 standard deviations is visible, shifted by 0.04° toward the West and 0.14° toward the North with respect to the nominal Moon position [3].

The projection of the deficit along the North-South axis, where the magnetic deflection is expected to be negligible, can be fitted by a Gauss distribution with a width in good agreement with the expected angular resolution.

Using a Montecarlo that simulates the path of the cosmic rays in the geomagnetic field, the position of the Moon shadow is expected to be shifted toward the West by $\sim 0.3^\circ$, due to the magnetic deflection. The observed position of the shadow shows a diplacement of $\sim 0.25^\circ$ with respect to the expected position. The systematics causing this shift are currently under investigation.

Also the Sun casts a shadow on cosmic rays, but sometimes the effects of its highly variable magnetic field are so strong to hamper the observation of the shadow. However in 2006 the solar activity was at its minimum and the

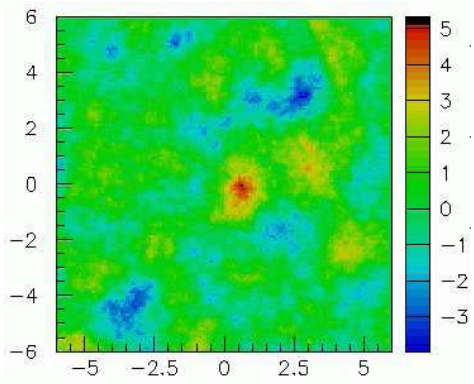

Figure 6: Map of the Crab Nebula region. The colour scale shows the significance of the signal in standard deviations. The axes report the distance in degrees from the source position.

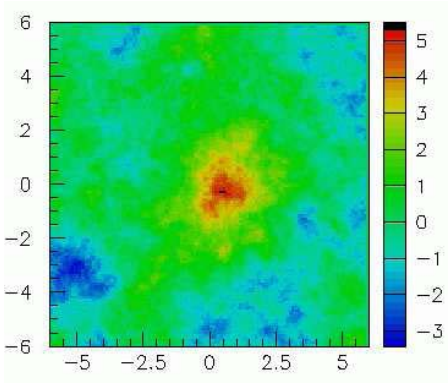

Figure 7: Map of the Mrk421 region during the outburst of July-August 2006. The colour scale shows the significance of the signal in standard deviations. The axes report the distance in degrees from the source position.

Sun shadow appeared with a statistical significance of more than 6 standard deviations, as shown in the map of Fig. 5 obtained in 208 hours of observation.

4 Gamma Ray sources

Among the steady TeV gamma ray sources, the Crab Nebula is the most luminous and it is used as a standard candle to check the detectors sensitivity.

Fig. 6 shows the map of the Crab Nebula region obtained by ARGO-YBJ using the events with $N_{pad} \geq 200$ and zenith angle $< 40°$ recorded in 290 hours of observation, equivalent to $\sim$50 transits of the source (one transit lasts 5.8 hours). The Crab is visible with a significance of more than 5 standard deviations.

In July-August 2006 the AGN Markarian 421 underwent an active period, with a rather strong increase of the X-ray flux[4]. As observed in many occasions during the past years, the X-ray flux increases are generally associated to increases in the TeV band, that can reach a flux several times larger than the Crab Nebula one. The 2006 summer outburst was not observable by Cherenkov telescopes, being the source high in the sky during the daytime.

ARGO-YBJ observed Mrk421 for 80 hours in July and August, during a debugging phase of the detector, just at the end of the installation of the central carpet.

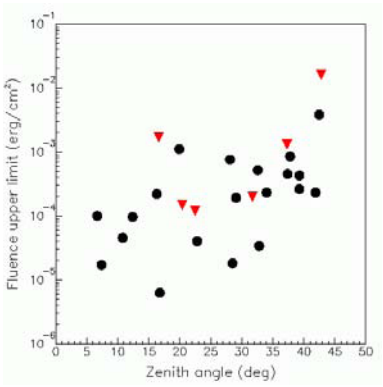

Figure 8: Fluence upper limits for 26 GRBs in the energy range 1-100 GeV, as a function of the zenith angle. The values shown by red triangles have been corrected for the absorption of gamma rays in the extragalactic space.

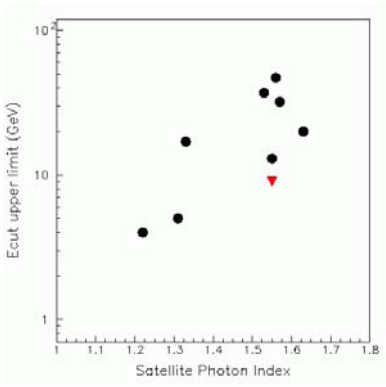

Figure 9: Upper limits to the maximum energy of GRBs spectra. The values shown by red triangles have been corrected for the absorption of gamma rays in the extragalactic space.

Fig. 7 shows the map of the region around the source, obtained with the events with $N_{pad} \geq 60$ and zenith angle $< 40°$. The significance of the signal is more than 5 standard deviations. Considering the low threshold used in this analysis, the detected emission is mostly at energies lower than 1 TeV. A more accurate evaluation of the energies is in progress.

The position of both the Crab Nebula and Mrk421 signals appears slightly shifted eastward with respect to the sources nominal position. The causes of this shift are under study.

5 Gamma Ray Bursts

The scaler mode technique offers a unique tool to study GRBs in the GeV energy range, where gamma rays are less affected by the absorption due to pair production in the extragalactic space[5].

The search has been done in coincidence with 26 GRBs detected by satellites (mainly by Swift). No excess has been found neither in coincidence with the low energy detection, nor in an interval of 2 hours around it [6].

Fig. 8 shows the fluence upper limits for the 26 GRBs in the energy range 1-100 GeV during the satellite time detection, as a function of the zenith angle, obtained assuming a power law spectrum with an index α=-2.5. When the

GRB distance is measured, the spectra are corrected with a factor that takes into account the extragalactic absorption[7].

Fig. 9 shows the upper limits to the maximum energy of the GRB spectra, obtained extrapolating with the same slope the power law spectrum measured by satellites. In some cases the limits are less than 10 GeV.

6 Conclusions

The central carpet of ARGO-YBJ has been installed and is taking data since July 2006. The data recorded in the first months of measurement have been analyzed in order to test the performance of the detector in the gamma ray astronomy field. The detection of the Moon and Sun shadows, together with a preliminary observation of a gamma ray flux from the Crab Nebula and Mrk421, show that the detector is properly working, with excellent angular resolution and sensitivity.

Working in "scaler mode" ARGO-YBJ has also performed a search for emission from GRBs in coincidence with 26 events observed by satellites, setting upper limits on the fluence between 6×10^{-6} and 2×10^{-2} erg cm^{-2} in the 1-100 GeV energy range.

A further increase of the sensitivity to gamma rays is expected with the installation of a converter layer of lead above the detector, and after the implementation of an offline procedure to reject a fraction of the cosmic ray background, based on the different topological pattern of hadronic and electromagnetic showers.

References

[1] H.H. He et al., *Astroparticle Physics 27, 528-532 (2007)*

[2] G. Di Sciascio et al. *Proc. 30th Int. Cosmic Rays Conference (2007)*

[3] B. Wang et al., *Proc. 30th Int. Cosmic Rays Conference (2007)*

[4] http://xte.mit.edu/

[5] S. Vernetto, *Astroparticle Physics, 13, 75 (2000)*

[6] T. Di Girolamo et al., *Proc. 30th Int. Cosmic Rays Conference (2007)*

[7] T.M. Kneiske et al., *Astronomy and Astrophysics, 413, 807 (2004)*